Green Mountains and White Plains: The Effect of Northern Hemisphere Ice Sheets on the Global Energy Budget

WILLIAM H. G. ROBERTS AND PAUL J. VALDES

School of Geographical Sciences, University of Bristol, Bristol, United Kingdom

(Manuscript received 26 November 2015, in final form 16 December 2016)

ABSTRACT

The changes in the global energy budget in response to imposing an ice sheet's topography, albedo, or topography and albedo combined are examined. The albedo of the ice sheet (here called a ''White Plain'') causes an outgoing top of the atmosphere radiation anomaly over the ice sheet that is balanced by an incoming anomaly in the Southern Hemisphere. This causes a northward transport of heat across the equator that is carried equally by the ocean and atmosphere. The topography of the ice sheet (''Green Mountain'') causes an incoming radiation anomaly over the ice sheet that is balanced predominantly by an outgoing anomaly to the south of the ice sheet, with a smaller outgoing flux in the Southern Hemisphere. The heat is transported across the equator by the atmosphere alone. The combined topography and albedo of the ice sheet (''White Mountain'') cause an outgoing radiation anomaly over the ice sheet that is balanced equally by an incoming flux in the Southern Hemisphere and to the south of the ice sheet. Heat is transported across the equator by the ocean alone.

With varying ice sheet geometry generally linear relationships between the various energy fluxes and the varying height and area of the ice sheet are found. In both the White Plain and White Mountain cases the ocean is always a significant carrier of heat across the equator, and in the White Mountain case it is preeminent.

1. Introduction

During glacial times the global climate was quite different from that which we observe today. Of the large-scale causes of this change, much has been written about the effect of greenhouse gases (e.g., Hansen et al. 1984) and varying orbital forcing (e.g., Phillipps and Held 1994); less, however, has been written considering the effect that the large ice sheets may play, especially when the ice sheets are relatively small. While the local effects of the ice sheet on the midlatitude circulation have long been considered (e.g., Cook and Held 1988; Kutzbach and Wright 1985), their global impact has been somewhat ignored and never examined with a fully coupled ocean–atmosphere climate model (Manabe and Broccoli 1985). There has been much written recently about the effect that changing the contrast between the temperature and energy balance in the Northern and Southern Hemispheres can have on the position of tropical rain belts and transports of energy across the equator (e.g., Yoshimori and Broccoli 2008; Kang et al. 2008; Chiang and Friedman 2012; Donohoe et al. 2013). This framework has proven itself quite useful for understanding changes in the large-scale circulation. Because glacial ice sheets are a major presence only in the Northern Hemisphere (NH), they are a likely candidate for setting up contrasts between the hemispheres. Therefore we might be able to use this framework to explain changes in the large-scale climate during glacial periods. However, before we can make use of this framework we must first understand what it is about the ice sheets that causes there to be a change in the interhemispheric energy balance. This is what we shall investigate in this paper.

It is clear that at the Last Glacial Maximum (LGM), the presence of an ice sheet in the NH can cause a cooling in this hemisphere (Hansen et al. 1984; Manabe and Broccoli 1985). It is not clear, however, what feature of the ice sheet it is that causes this cooling. Increasing the albedo of the surface, as happens when ice accumulates, causes a reduction in the incoming shortwave radiation and thus a cooling of the surface (Hansen et al. 1984; Broccoli and Manabe 1987; Rind 1987; Felzer et al. 1996; Justino et al. 2005; Pausata et al. 2011). But, as ice

Corresponding author e-mail: William H. G. Roberts, william.roberts@bristol.ac.uk

DOI: 10.1175/JCLI-D-15-0846.1

accumulates the surface elevation also changes and so too can the climate's response (Kageyama and Valdes 2000; Hofer et al. 2012; Ullman et al. 2014). Although many studies report that with an increase in elevation the surface cools, it is unclear whether this cooling is due merely to lapse rate effects, to the fact that a higher surface will be cooler, or to additional feedbacks that alter the climate's energy balance, particularly those that reduce the amount of energy incident at the surface. Slab model experiments in which the topography and albedo are changed individually (Chiang et al. 2003) show that there are feedbacks that can alter the response of the atmosphere to an ice sheet: they also emphasize the nonlinearity of these feedbacks highlighting the differences between an albedo-alone response and a topography-alone response.

If the climate is at a radiative equilibrium, with the global incoming and outgoing TOA radiation balanced, any increase in the outgoing radiation, from, for example, an increase in the surface albedo must be balanced by either an increase in the incoming radiation or a decrease in the outgoing radiation somewhere else. This change could happen globally, by, for example, a global cooling and reduction in the global outgoing longwave radiation, or locally, by, for example, a reduction in the amount of high tropical clouds and thus reduction in the local OLR. These both imply some sort of heat transport from the region of net incoming radiation to that of net outgoing and, in the latter case especially, if the change occurs in the SH this implies a heat transport across the equator. Therefore, we can potentially explain the cross-equatorial heat transport that arises from a cooling at high latitudes caused by a radiative imbalance at the TOA, as a necessary part of balancing the TOA heat budget.

The importance of moving heat from one hemisphere to another in response to a hemispheric cooling has been emphasized in a number of studies (Kang et al. 2008; Cvijanovic and Chiang 2013). Although these studies do show that when the high latitudes are cooled there is a change in the cross-equatorial heat transport, there are a number of problems if we wish to relate these studies to how the climate responds to an ice sheet. Most importantly, they all prescribe some change in the surface energy balance and assess the climate's response to this. If an ice sheet grows, the climate responds to the change in the boundary conditions and part of this response is the change in the surface energy balance. Therefore, without knowing how the surface energy balance responds to an ice sheet, we cannot say whether the imposed heat fluxes of the simple experiments are a suitable analog. More concretely, does the growth of an ice sheet imply changes in the ocean heat transport that are similar to those implied by cooling the high latitudes in a slab ocean model? Furthermore, as we have discussed previously, do changes in the surface topography cause changes in the circulation that are sufficiently large to confuse inferences made from simulations in which the topography does not change?

Of course, as an ice sheet evolves there is no reason to expect that the relative importance of the ice sheet topography and albedo will remain the same. A number of sets of simulations have shown that as an ice sheet's topography changes so does its impact on the climate (Chiang et al. 2003; Li and Battisti 2008; Lee et al. 2015; Ullman et al. 2014). It is likely that such effects on the climate imply some changes in the climate's energy balance. These simulations have examined the effect of varying topographic height, in isolation: in all cases the surface area of the ice sheet was kept constant. As an ice sheet grows and decays its surface area will also grow and decay, and so the albedo effect on the climate will also change. Experiments that assume that the ice sheet's area is similar to the LGM are likely suitable for simulating marine isotope stage 3 (MIS3) until the LGM (Kleman et al. 2013); however, for other periods when the ice sheet was markedly smaller, such simulations will overestimate the ice sheets area and potentially the influence that albedo will play in the climate's response. Thus if we are to understand how the energy balance over an ice sheet changes on long time scales we must change the area, and hence the albedo, of the ice sheet along with its topography.

In this study we shall investigate some of these questions. We shall examine how the energy balance over an ice sheet is affected by the topography and albedo of the ice sheet with each effect taken in isolation and in concert. We shall then examine how the global TOA energy balance is affected by the imposition of the ice sheet, to understand whether any compensating energy fluxes have a preferred location.

We shall examine how any energy is transported across the equator, asking if it goes through the ocean or the atmosphere. Finally we shall investigate how the balance of energy terms varies with a time-evolving ice sheet. To do this we use a reconstruction of the Laurentide Ice Sheet (LIS) from 21 ka (i.e., 21 000 years ago) to 6 ka. This reconstruction simulates changes in both the area and topography of the ice sheet.

Section 2 describes the model setup and experiments. Section 3 describes the energy balance over the ice sheet when the ice sheet is at its largest and in section 4 we describe the global top-of-atmosphere (TOA) energy balance and the equatorial heat transports. Section 5 describes how the global TOA energy budget evolves

when we use the ice sheet reconstruction. Finally, we conclude in section 6.

2. Model configuration

We use the global climate model HadCM3 for all of our simulations (Gordon et al. 2000). Although it can no longer be considered a ''state of the art'' climate model, HadCM3 has a number of benefits over more modern climate models. First, because of its age, numerous studies have shown its successes and failures in simulating the climate so its biases, such as a double-ITCZ and too extensive a Pacific cold tongue, are well understood (e.g., Toniazzo et al. 2008; Spencer et al. 2007). Second, because of its relatively low resolution, by modern standards, for a full-complexity GCM it is relatively quick to run, and therefore many long simulations can be made. Being able to make long simulations means that we can approach some sort of equilibrium in the climate, although this is not assured; being able to make numerous runs means we can analyze trends in the climate's response to incremental changes in the forcing. Furthermore, being able to replicate results with slightly different boundary conditions gives us confidence that the response of the climate model that we see is indeed a forced response and not an artifact of a particular initial condition.

We derive our boundary conditions from the ICE-5G (VM2) model reconstruction of the ice sheets (Peltier 2004). Unless otherwise indicated, boundary conditions are for preindustrial values. This includes the greenhouse gases and orbital forcing and the land–sea mask. Of course, over the Last Deglaciation all of these forcings changed, but it is not our intention to make the best simulation of the Last Deglaciation but rather to understand how an ice sheet impacts the climate. We simulate time slices every 1 ka from 21 ka until 6 ka.

To investigate the effect of albedo (experiment ALB), land areas that are ice covered at each time slices have all of their surface properties set to those of land ice. These include surface albedo and roughness, and all of the model's other vegetation and soil parameters. We impose this land surface change to all ice-covered areas in the Northern Hemisphere and so include changes in the albedo over both North America, where the LIS lay, and over northern Europe, where the Eurasian Ice Sheet lay. In this way we create a time-varying ''White Plain'' in the NH.

To investigate the role of topography (experiment TOP), land areas in which the LIS existed have their surface topography raised to be that of the ice5g reconstruction. We add this surface elevation change as an anomaly to the preindustrial topography that is used in control runs of HadCM3. We only change the surface topography over North America; everywhere else remains as in the preindustrial. We therefore ignore the effect of the Eurasian Ice Sheet's topography. Because of its larger size the LIS has a much larger impact on the climate than the Eurasian Ice Sheet. All other surface properties remain the same as for the preindustrial. It should be noted that over time, because of the increased elevation of the surface, snow does accumulate on top of the topography anomaly causing a small albedo anomaly. It can be seen (Figs. 9b and 9d) that there is a small change in the ice sheet area in experiment TOP; the figures also show that this change is a tiny fraction of the change in the albedo that arises from the imposition of an ice sheet. With these changes in the surface properties we create a ''Green Mountain.''

Finally to investigate the role of topography and albedo (experiment ALB/TOP) we combine the boundary condition changes of experiments ALB and TOP. We therefore have a land surface that simulates land ice, and its associated change in albedo, everywhere that was ice covered in the NH at each time slice (including over Eurasia), and a topography that is raised over North America (but not over Eurasia). In this way we create a ''White Mountain.''

The land–sea mask that we use is for the preindustrial. We therefore ignore any land area changes that arises from the drop in sea level as land ice accumulates. This has a number of implications. First, because much of the land exposed during the LGM lies in high northern latitudes, and therefore would have been ice and snow covered during the LGM, the 21ka albedo anomaly that we impose is smaller than that at the LGM. Simulations that include this change in the land area, and increased change in the albedo relative to the preindustrial land sea mask, fit with the trends that we see (see Fig. 9), but with commensurately larger changes in the energy fluxes. Second, at the LGM some of these land areas had accumulated enough ice to change the surface elevation. These additional areas of elevation we ignore. They are generally small and at the margins of the ice sheet and so have little impact on the change in the circulation. Finally, as the sea level dropped, what is now Hudson Bay was land, and indeed sometimes ice-covered land. In all experiments we include this effect by removing Hudson Bay and turning it to land. This includes times during the last deglaciation when Hudson Bay was in fact ocean. At these times we set the land surface to be ice-free land with similar properties to adjoining ice-free land and with zero elevation.

We wish to understand what the long-term response of the climate is to the ice sheet, and therefore we need our model simulations to be near equilibrium. With a fully coupled climate model, achieving true equilibrium

is almost impossible without prohibitively long simulations. We therefore run our simulations for long enough that any energy imbalance is small, and will not affect our results. The detailed analyses of the 21ka experiments (sections 3 and 4) all use simulations run for 700 years (ALB, TOP) or 900 years (ALB/TOP), with results presented for averages over the final 100 years. For the time-varying simulations over 21ka to 6 ka (section 5) we present results from models that have been run for 200 years (ALB) or 500 years (TOP, ALB/TOP), with results presented for averages over the final 100 years. All statistics are derived from annual mean quantities. We must note that over a typical glacial cycle, the climate is never truly at equilibrium with its forcing, since the forcing typically changes on a time scale longer than the time it takes for the deep ocean to adjust. The ~500-yr time scale that we investigate here is typical of the time scale for the climate to adjust to its forcing—over the last deglaciation the Laurentide Ice Sheet took ~10 000 years to disappear.

By the end of the long 21ka simulations the average energy imbalance at the top of the atmosphere in each simulation is around 0.15 PW ($0.3\,W\,m^{-2}$; see Fig. 1). This is sufficiently small compared to the average incoming radiation flux of $341.4\,W\,m^{-2}$ that we can consider that the model is at equilibrium and the majority of the adjustment has taken place. We note that the TOA imbalance in the PMIP2 simulations, which have been used to study the energetics of the atmosphere in glacial times (Donohoe et al. 2013), has a range from 0.2 to $1.6\,W\,m^{-2}$. Our simulations are therefore no further from equilibrium than other similar modeling studies.

This is not to say that the energy imbalance is irrelevant; indeed, in some cases total energy imbalance is of a similar size to some of the TOA fluxes that we investigate. We show in Table 1 how large this imbalance is and make no effort to remove this bias from any of our results. (This means that in Fig. 4 the TOA fluxes do not sum to zero.) That the model is not fully spun up does call into question our results. However, we find that the relative importance of each of the area-integrated fluxes we present does not change after 100 years of simulation. Figure 1 shows the annual averaged output over the full spinup of the 21ka simulations. It is clear from this figure that although it takes up to 700 years after the imposition of the ice sheet forcing for the total TOA energy flux imbalance to become negligible (Fig. 1a), it takes less than 200 years for the regional patterns of change to become established (Figs. 1b–d). Indeed, we can see in Fig. 1 that all of the conclusions that we draw in sections 2 and 3 could just as well have been drawn after 200 years of simulation as after 900. The exact magnitude of the energy flux anomalies that we report will change, but the predominance of one term over another would be no different. It is also worth noting that there is significant decadal variability in the modeled fluxes. Taking 100-yr means (darker lines in Fig. 1) eliminates some, but not all, of this variability. Taking 50-yr means (lighter lines) fails to remove this variability. However, the changes in the fluxes that we simulate are, again, large enough to negate any impact from this and our overall conclusions using 50-yr means would be the same as using 100-yr means.

TABLE 1. TOA net heat fluxes and cross-equatorial heat transports. The net TOA heat fluxes are integrated in a number of latitude bands, the extent of which are shown in the text; positive values indicate an outgoing heat flux. The implied cross-equatorial atmosphere and ocean heat fluxes are shown in *italics*; positive values indicate northward heat transports. All units are in PW. (ALB and TOP values are for the final 100 yr of a 700-yr run; ALB/TOP values are for the final 100 yr of a 900-yr run.)

	Term	ALB	TOP	ALB/TOP
TOA	Ice Sheet	0.36	−0.24	0.22
	NTrop	−0.07	0.18	−0.09
	SHem	−0.22	0.10	−0.09
Surface	Ice Sheet	0.06	0.14	0.26
	NTrop	0.07	−0.06	−0.20
	SHem	−0.12	−0.01	−0.10
	Total	0.03	0.03	0.01
	Atmosphere	*0.11*	*−0.10*	*−0.01*
	Ocean	*0.12*	*0.02*	*0.10*

In our estimation of the interhemispheric heat transports we take residuals from the top of the atmosphere and surface energy budget. This is because calculating the exact energy budget terms from the model output requires output of variables on all model levels; this introduces a prohibitive storage overhead on the model simulations. As can be seen in Table 1 the total surface and TOA energy budgets are not equal, seeming to imply a convergence of energy in the atmosphere. This is not the case; rather, it is the case that the model diagnostics are insufficient to close the energy budget. This has the potential to introduce errors in the energy transport terms. Explicitly calculating the atmospheric heat transport on model levels for all of the 21ka simulations and comparing it with the residual calculation indicates that there is a negligible discrepancy between the two methods (not shown). We therefore use the residual method. In the ocean however, the imbalance in the incoming and outgoing radiation flux indicates that the ocean is cooling over all of our simulations. This is expressed in the TOA imbalance discussed above. Without running our simulations for still longer, this term cannot be eliminated. Therefore, we state here that there is the potential that after even longer integration the modeled heat transport may still change. Readers should bear in mind, however, that over a glacial cycle the climate

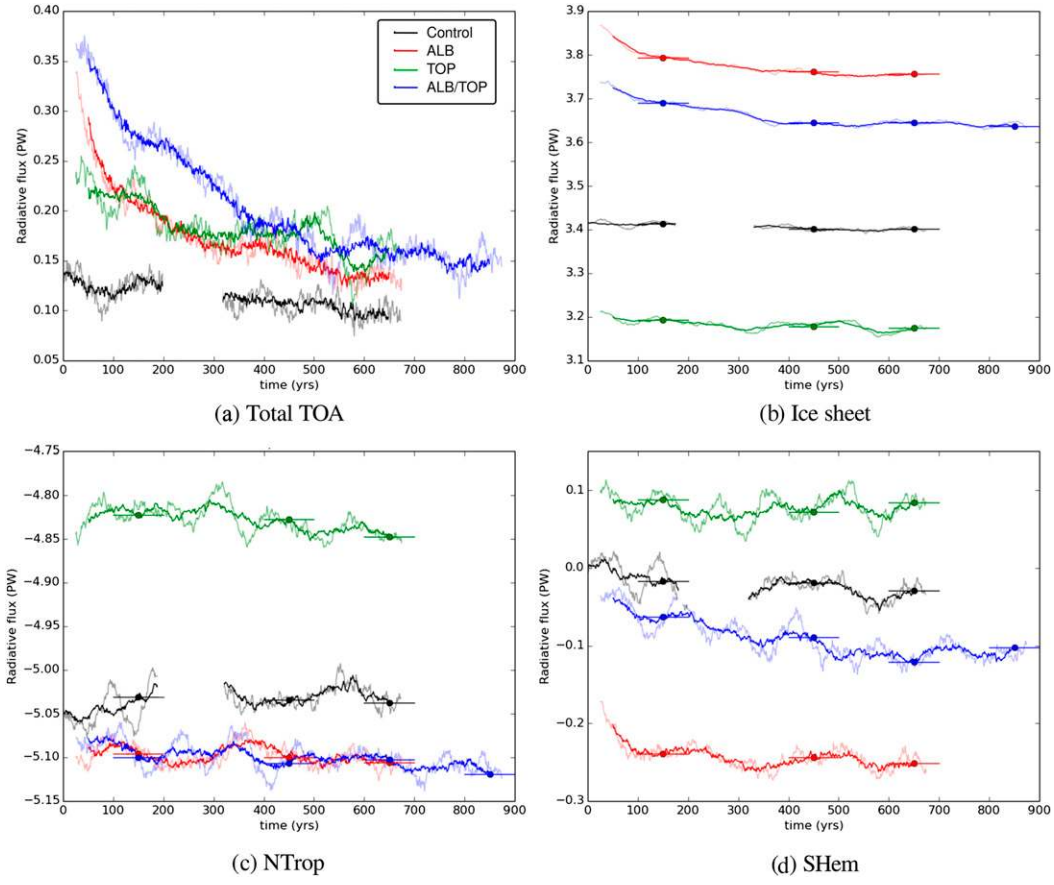

FIG. 1. Zonally integrated top of the atmosphere (TOA) radiation in four regions: (a) global average, (b) over the ice sheet, (c) in the Northern Hemisphere south of the ice sheet, and (d) in the Southern Hemisphere. The darker (lighter) lines show 100-yr (50 yr) running means; dots show the 100-yr averages after 200, 500, 700, and 900 years of simulation. Black line is the control, red the White Mountain (ALB), green the Green Mountain (TOP), and blue the White Mountain (ALB/TOP).

system is never likely to be in equilibrium with its forcing, and the response in the surface and intermediate ocean that we can simulate over the ~500-yr time scale presented here is typical of the climate's response to ice sheet forcing.

In all figures and tables we report the TOA energy fluxes as positive upward: a positive flux is therefore an outgoing energy flux. The total horizontal heat transport is calculated by integrating the net zonally integrated TOA energy flux over latitude. The atmospheric component is calculated as the integral of the difference between the net TOA radiation and the net surface energy flux over latitude, and the ocean component is calculated as the residual of the total and atmospheric components. Horizontal heat transports are reported as positive northward.

3. TOA energy budget over the ice sheet at 21 ka

Figure 2b shows the net zonally integrated TOA radiation anomaly calculated for the long 21ka runs relative to the control, shown in Fig. 2a. We see that over the ice sheet (between the vertical dash-dotted lines at 45°–70°N) there is a change in the net TOA radiation. In the simulations in which the albedo of the surface is changed, ALB and ALB/TOP, there is a net reduction in the amount of radiation entering the top of the atmosphere. In ALB this reduction happens only over the regions in which the ice sheet is located; in ALB/TOP there is a reduction as far south as 35°N, far to the south of the ice sheet's southern edge. The change in TOA radiation over the ice sheet is of a similar magnitude in ALB and ALB/TOP, though somewhat smaller in ALB/TOP. By contrast in TOP there is an increase in the amount of energy entering at the TOA over the ice sheet.

A change in the TOA radiation can be brought about by a change in either the outgoing longwave radiation or the net shortwave radiation. We show in Figs. 2c and 2d these terms. We see that in ALB there is an increase in

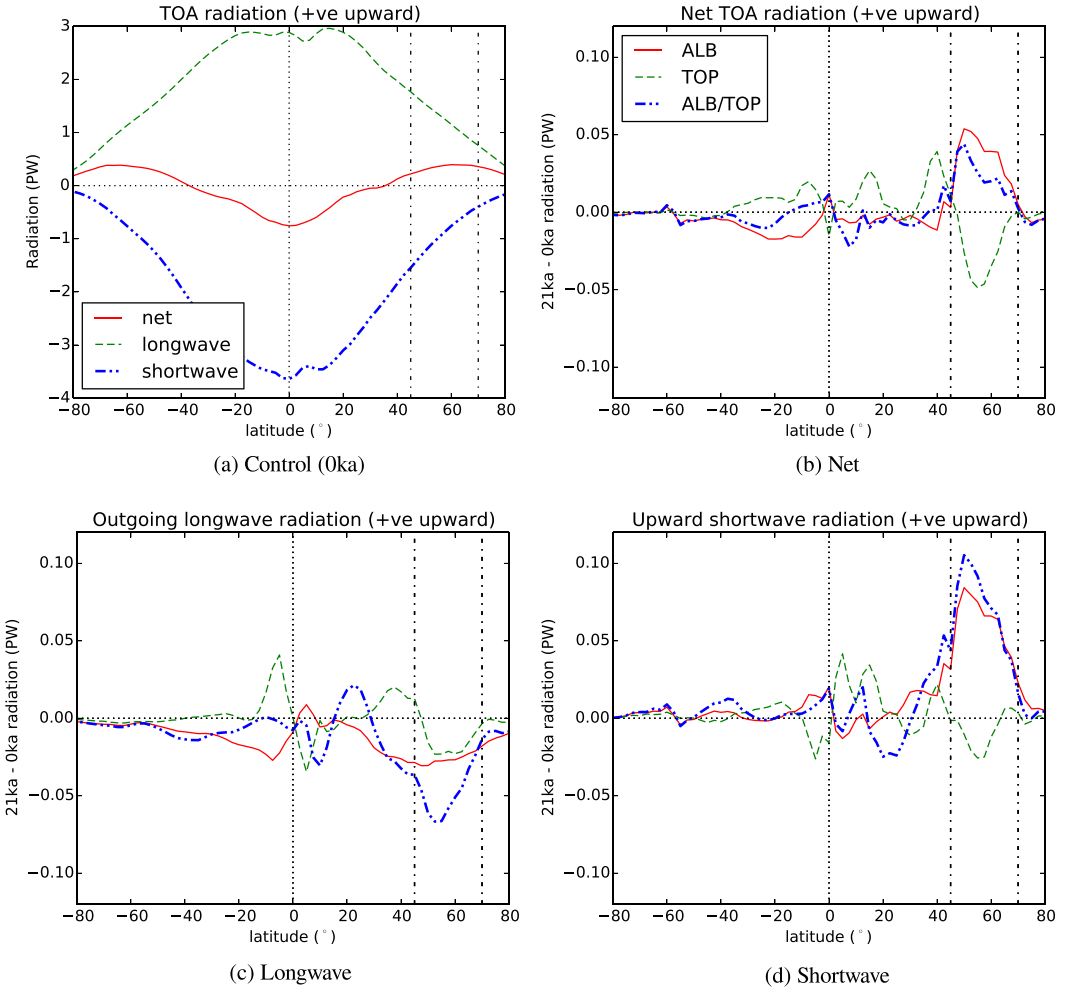

FIG. 2. Zonally integrated TOA radiation: (a) the preindustrial (0 ka) TOA radiative fluxes and (b)–(d) the differences between a 21ka simulation and the preindustrial control for the net, longwave, and shortwave radiation, respectively. The solid red line shows results for experiment ALB, dashed blue line is TOP, and dash-dotted green line is ALB/TOP.

the outgoing shortwave radiation over the ice sheet. This increase is offset by a decrease in the outgoing longwave radiation caused by the cooling of the atmosphere over the ice sheet. It is interesting to note that the anomalies in the short and longwave fluxes both extend far to the south of the ice sheet, but south of the ice edge the outgoing shortwave anomaly nearly cancels the longwave anomaly with the resulting net flux near zero. Thus, in the net, we only see the largest change in the TOA radiation directly over the ice sheet. We shall discuss the small changes remote from the ice sheet in subsequent sections.

The TOA shortwave radiation is determined by the planetary albedo. This has two components: one due to reflections from the surface and one due to reflections from the atmosphere. In the global mean this latter term is the largest (Donohoe and Battisti 2011). Following Donohoe and Battisti (2011) we decompose the planetary albedo into these two components. This method assumes that of the incident solar radiation S, a fraction A is absorbed by the atmosphere and a fraction R is reflected. Of this reflected fraction a further fraction A is absorbed and fraction R reflected and so on. Thus the total shortwave radiation at the TOA can be expressed as an infinite sum of the fractions A and R multiplied by S. Similarly the surface shortwave radiation can also be expressed in terms of A and R. Therefore, since we know S, the outgoing TOA and surface shortwave radiation at each point we can solve for A and R around the globe. Finally, from A and R we can obtain expressions for the surface and atmospheric albedo. Full mathematical detail is contained within Donohoe and Battisti (2011).

In Fig. 3 we see that in ALB the change in the TOA shortwave radiative flux over the ice sheet is caused

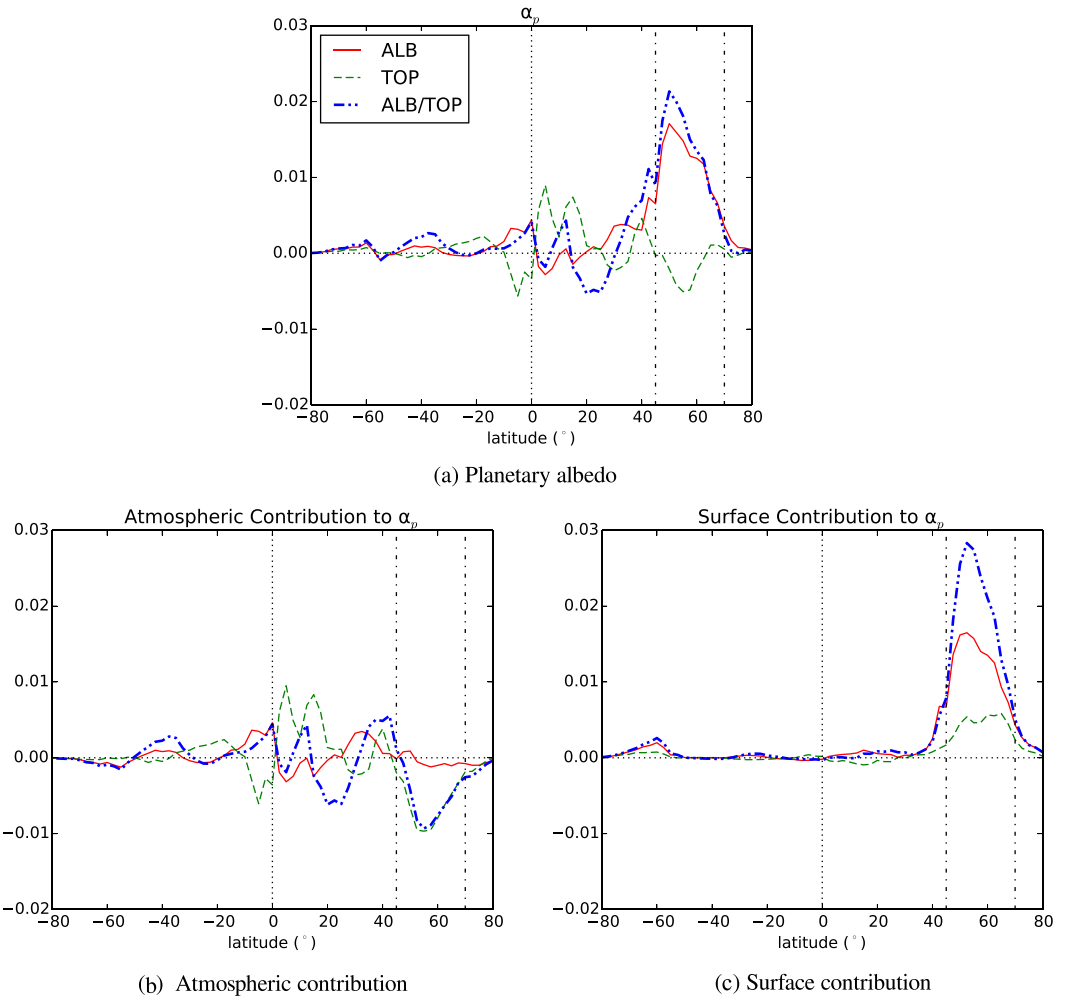

(a) Planetary albedo

(b) Atmospheric contribution

(c) Surface contribution

FIG. 3. Zonally averaged TOA planetary albedo. (a) Differences between a 21ka simulation and the preindustrial control, and the albedo decomposed into the contributions from (b) the change in the atmospheric reflectivity and (c) the change in the surface albedo. The solid red line shows results for experiment ALB, dashed blue line for TOP, and dash-dotted green line for ALB/TOP.

almost entirely by changing the surface albedo with a negligible effect from the atmosphere. The shortwave energy flux change is thus a direct response to the imposed albedo anomaly. To the south of the ice sheet, however, it is the change in the atmospheric component of the albedo that gives rise to the change in the TOA shortwave radiation.

The reduction in the outgoing longwave radiation over the ice sheet is the result of a general cooling of the atmospheric column over the ice sheet. At the surface we see little change in the energy flux. Over the ice sheet this is because the increase in the upward shortwave radiation is balanced by a decrease in the latent, longwave, and sensible heat fluxes. These compensating decreases are all caused by the cooling of the surface. We cannot, therefore, directly couch the changes in the TOA radiation balance in terms of the change in the surface energy budget.

In TOP both the outgoing shortwave and outgoing longwave radiation terms are reduced over the ice sheet. We find that the decrease in the shortwave flux is due to a change in the atmospheric circulation that acts to decrease the atmospheric contribution to the planetary albedo (Fig. 3). Raising the surface of the earth does increase the surface component of the albedo, because relative to the control topography there is less atmosphere between the surface and the TOA, but this effect is not sufficient to counteract the decrease in albedo caused by the atmosphere itself. The reduction in the OLR over the ice sheet is the result of a reduction in the humidity over the ice sheet; the column averaged temperature is little changed by the imposition of the ice sheet.

At the surface there is an increase in the upward energy flux. This is the result of a flux of heat out of the oceans. Over the ice sheet itself there is a negligible

change in the surface heat flux. This is because the changes in the shortwave radiation flux at the surface are balanced by changes in the longwave and sensible heat fluxes.

In ALB/TOP the outgoing shortwave radiation term is increased relative to the control, due to the increased albedo over the ice sheet. This increase is larger than that seen in ALB. We find that the cause of this is a larger surface albedo change in ALB/TOP than in ALB (Fig. 3). This is due to raising the surface of the earth closer to the TOA: a similar effect was seen in TOP. The change in the atmospheric circulation in ALB/TOP causes a reduction in the atmospheric contribution to the planetary albedo that reduces the overall increase in the planetary albedo somewhat, but not enough to compensate for the increase in the surface albedo. The atmospheric albedo change in ALB/TOP and TOP is very similar, indicating that changing the surface properties beneath the raised topography does not significantly alter this component; it is only caused by the physical effect of having an elevated surface and its attendant influence on the atmospheric circulation. There is a decrease in the outgoing longwave radiation in ALB/TOP due to both a reduction in the atmospheric temperature over the ice sheet (as in ALB) and a reduction in the humidity over the ice sheet (as in TOP). The resulting OLR anomaly is thus larger than that seen in TOP and ALB. Interestingly, the magnitude of the change in the column averaged temperature is similar in ALB and ALB/TOP, and the change in the humidity is of a similar size in TOP and ALB/TOP. The resulting change in the OLR over the ice is then close to the linear sum of these two effects. This can be seen in Fig. 2c where over the ice sheet the change in the OLR in ALB/TOP is approximately the sum of that in ALB and that in TOP.

In sum, the decrease in the OLR in ALB/TOP is larger than the increase in the shortwave, meaning that the net TOA flux in ALB/TOP is slightly less, although comparable to ALB. Therefore, although there are additional feedbacks that amplify the change in both the longwave and shortwave radiation in ALB/TOP compared to ALB, these feedbacks do tend to cancel each other out.

At the surface we find that there is a large increase in the upward heat flux in ALB/TOP. This is the result of a large flux of heat out of the oceans. Over the ice sheet there is a negligible change in the heat flux because the increased upward shortwave heat flux is balanced by a decrease in the longwave, latent, and sensible heat fluxes. This reduction is due to the cooling of the surface.

We have shown that the imposition of the ice sheet boundary conditions causes a change in the TOA radiation budget over the ice sheet in comparison to the preindustrial. Such changes in the TOA radiation budget imply one of two things: either the climate must cool or warm to balance this change or, if the climate remains at the same temperature, there must be a change in the heat transport in the climate to balance the loss of energy over the ice sheet with a gain elsewhere, or vice versa. We shall investigate this in the next section.

4. Global TOA energy budget at 21 ka

We can see in Fig. 2 that there are changes in the TOA radiation budget away from the ice sheet and that there is a large amount of latitudinal structure to these. To categorize these broadscale changes we present in Table 1 and Fig. 4 the TOA energy changes relative to the control, integrated over a number of latitude bands: the Ice Sheet (45°–70°N), the northern tropics (NTrop; 0°–45°N), and the Southern Hemisphere (SHem; 0°–90°S). We can thus assess whether the change in the radiation budget over the ice sheet is balanced by a compensating TOA flux to the south of, but in the same hemisphere as, the ice sheet (NTrop) or into the SH (SHem). If the compensating flux is in the SH this implies that there must be a cross-equatorial energy flux—such a flux may imply movements of the ITCZ (Kang et al. 2008). We summarize these results in Fig. 4. We also include the implied cross-equatorial heat fluxes, derived from the net TOA and surface energy budgets.

a. ALB

In experiment ALB we see that the radiative flux out of the atmosphere over the ice sheet is balanced predominantly by a flux of energy into the atmosphere in SHem. There is also a small flux into the TOA in NTrop. In SHem the decrease in the net outgoing TOA flux is caused by a reduction in the outgoing longwave radiation. This decrease in the longwave flux is, to some degree, compensated by an increase in the upward shortwave flux. This opposition between changes in the long and shortwave radiation is a common feature of the climate's response to the ice sheets. Within the model, in the tropical regions a decrease in the upward longwave radiation is associated with an increase in the amount of high clouds, cooling the upper atmosphere. In turn, the processes that give more high clouds tend to also give more low clouds; these increase the albedo and thus increase the upward shortwave radiation. Therefore the processes that decrease the outgoing longwave radiation tend to increase the outgoing shortwave radiation and thus there is little change in the net. In this way, the regions in which there are the largest changes in the net radiation are not necessarily the regions that experience the largest changes in the longwave and shortwave

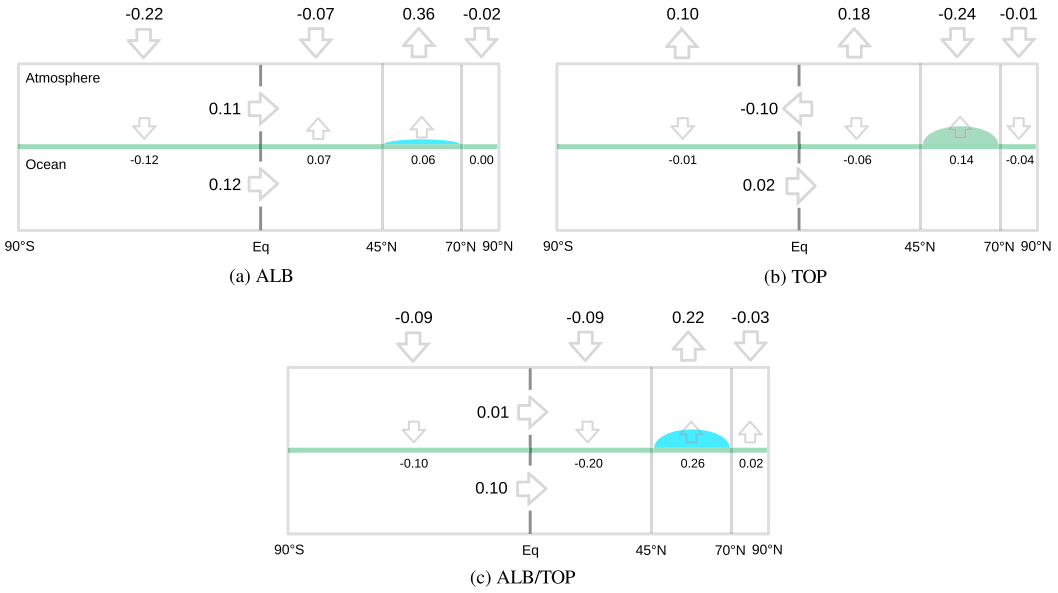

FIG. 4. Schematic of TOA energy flux and inferred cross-equatorial heat fluxes. All units are PW.

radiation. The regions that we find are responsible for the changes in net energy flux in SHem are the equatorial Atlantic and globally south 15°S (Fig. 5a). In both of these regions the reduced outgoing longwave radiation that results from increased upper-level clouds is not balanced by an increase in the lower-level clouds with the attendant increase in the outgoing shortwave radiation (Fig. 6a). Indeed in the Atlantic there is a *decrease* in the amount of low cloud where the high cloud increases, causing a reduction in the upward shortwave radiation that reinforces the longwave changes.

In the region NTrop, there is a small incoming radiative flux that is approximately one-third the size of that in SHem. In the zonal mean this can be seen to be the result of a small difference between large changes in both the longwave and shortwave fluxes (Fig. 2). The majority of the change in the shortwave fluxes occurs in the Atlantic and in the east Pacific near 30°N (Fig. 6a). The changes in the longwave radiation are seen globally. The largest regional changes occur in the region of the ITCZ; however, the changes in the longwave and shortwave radiation tend to balance one another.

A flux of energy out of the atmosphere in the NH and a flux in over the SH implies that there is an increased energy flux across the equator from the south to the north. This tallies with previous studies that have shown that an increase in the albedo causes a change in the atmospheric energy transports, brought about by a change in the position of the zonal mean ITCZ (Chiang and Bitz 2005). Figure 4 shows that the heat transport across the equator is partitioned approximately equally between the atmosphere and the ocean. As we shall see later, the ratio of this split between the atmosphere and the ocean remains roughly constant regardless of the area of the ice sheet. Therefore, although we do find that an albedo anomaly in the high northern latitudes does imply a cross-equatorial heat transport, this does not have to be carried by the atmosphere alone.

In this experiment there is an increase in the strength of the ocean's Atlantic meridional overturning circulation (AMOC). This increase does little, however, to change the energy budget near the ice sheet. Figures 2 and 5a show that there is a negligible change in the surface energy flux at the latitude of the ice sheet. Therefore although the ocean transports more heat across the equator, this transport is not directly responsible for affecting the energy balance over the ice sheet.

b. TOP

Experiment TOP shows a quite different response. In this experiment we find that the decreased outgoing TOA energy flux over the ice sheet is balanced predominantly by an increased outgoing energy flux to the south of the ice sheet in NTrop. There is also a smaller increase in the outgoing radiation flux from SHem that is approximately half the size of that in NTrop.

In NTrop the increased outgoing radiation flux is again the result of changes in both the longwave and shortwave radiation (Fig. 6b). At the latitude of the southern edge of the ice sheet there are increases in the upward shortwave radiation in both the western Atlantic and western Pacific. There is also an increase in the upward longwave radiation upstream of sheet in the northeastern Pacific. In the equatorial regions there are large changes in both the

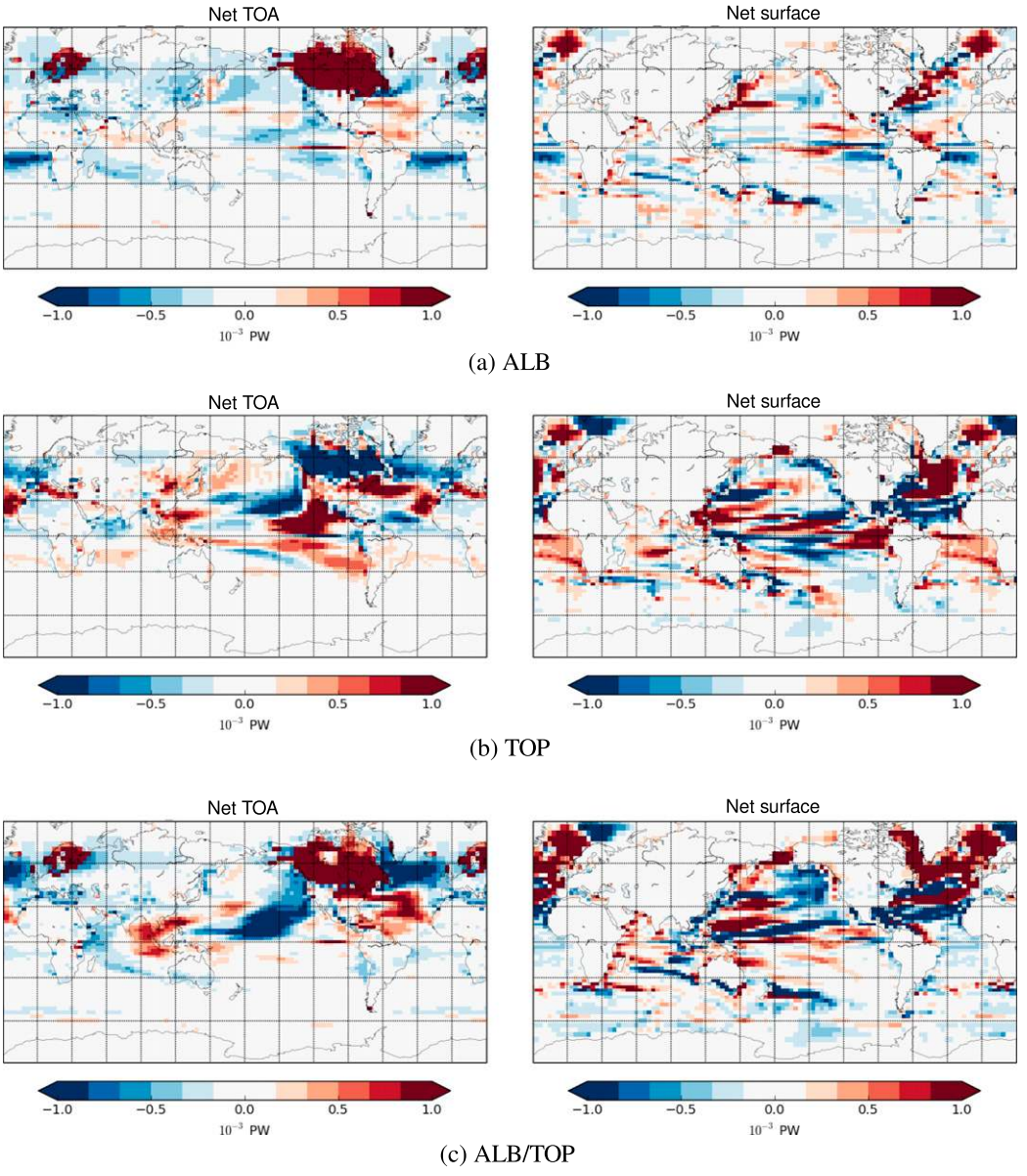

FIG. 5. Maps of the (left) net outgoing TOA and (right) upward surface radiation fluxes. Colors are plotted in 10^{-3} PW with colors changing every 0.25×10^{-3} PW.

longwave and shortwave radiation, with the shortwave terms dominating. These changes in the shortwave radiation are predominantly in the Pacific.

In SHem the increase in the upward radiation between 15°S and the equator is the result of increased upward longwave radiation in the east Pacific. South of this the increased upward radiation flux is in the shortwave and occurs globally. There are large changes in the south eastern tropical Pacific, but these changes tend to balance in the zonal mean.

Table 1 and Fig. 4 show that the SHem energy flux is accompanied by a southward energy flux across the equator. Almost all of this energy flux is accomplished by the atmosphere, with a negligible component in the ocean. The AMOC in this experiment is reduced somewhat, from 18.3 to 16.3 Sv ($1\,\mathrm{Sv} \equiv 10^6\,\mathrm{m^3\,s^{-1}}$), which suggests that any change in the ocean heat transport in the deep ocean is compensated for by changes in the shallow surface ocean circulation. As has been shown by Czaja and Marshall (2006) in the equatorial regions, there is significant ocean heat transport in the near surface. Thus in this experiment we find that the TOA radiation anomaly over the ice sheet is predominantly balanced in the same hemisphere as the forcing.

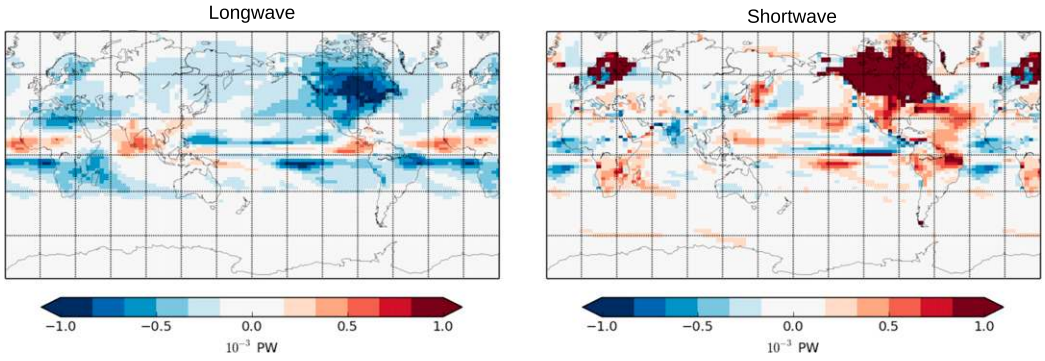

(a) ALB

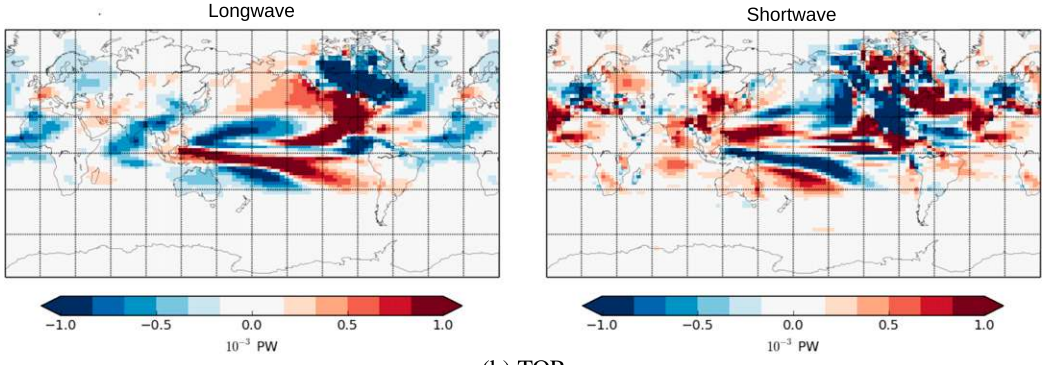

(b) TOP

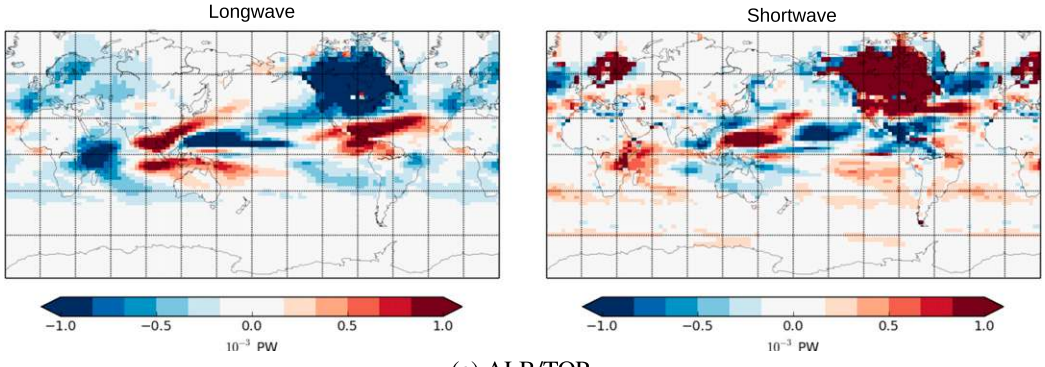

(c) ALB/TOP

FIG. 6. Maps of the TOA upward (left) longwave and (right) shortwave radiation fluxes. Colors are plotted in 10^{-3} PW with colors changing every 0.25×10^{-3} PW.

c. *ALB/TOP*

In experiment ALB/TOP the increased outgoing TOA radiation anomaly over the ice sheet is balanced by roughly equal fluxes into the atmosphere in both SHem and NTrop.

In SHem the incoming flux occurs principally in the longwave although there are also changes in the shortwave radiation that tend to oppose those in the longwave. South of 15°S there is a similarity between the response in ALB and ALB/TOP both in the zonal mean and regionally, with a reduction in the outgoing longwave radiation across all three ocean basins (Figs. 6a,c). Between the equator and 15°S ALB/TOP differs from ALB as the large longwave anomaly is absent. This is because the very large southward movement of the convection in the equatorial Atlantic in ALB is absent from ALB/TOP. A feature that is concealed by taking a zonal mean is the extremely large changes in the longwave and shortwave radiation in west Pacific and Indian Ocean. These are associated with an east–west movement of the convection in the tropics, which results in large local changes that cancel in the zonal mean.

In NTrop there is an incoming radiation anomaly that is the result of large changes in the long and shortwave radiation that nearly balance. This was also the case in ALB. The largest changes in the shortwave radiation occur in the Atlantic, as in ALB, and in western equatorial Atlantic. In the longwave the largest changes occur in the Indian Ocean and west Pacific, again this is associated with the large eastward movement of the convection in this region.

Figure 4 shows that although both ALB and ALB/TOP suggest a northward cross-equatorial heat flux, the means by which this is achieved is not the same. In ALB around half of the energy transport was accomplished by the atmosphere, whereas in ALB/TOP there is a negligible transport in the atmosphere. This suggests that either the changes in the topography affect the thermodynamics of the atmosphere such that it is less efficient at transporting energy or the topography affects the thermodynamics of the ocean such that it is more efficient at moving energy. With the present simulations we have no way of telling which. However, we recall that in TOP there was a southward atmospheric cross-equatorial heat transport and in ALB a northward transport. This hints, although in no way conclusively, that the combined response of ALB and TOP will be for no net heat transport by the atmosphere, thus leaving the ocean to carry the heat. Indeed it is interesting to note that the combined cross-equatorial heat flux response of ALB/TOP is the linear combination of the responses of ALB and TOP. In this experiment we find that the strength of the AMOC is dramatically increased from 18 to 25 Sv. Recall, however, that the cross-equatorial ocean heat transport in this experiment is very similar to that of ALB in which there was a small (0.8 Sv) increase in the AMOC. This echoes the results of experiment TOP that suggested that any change in the heat transported by the AMOC is but one constituent of the heat transported by the ocean and that changes in the shallow, wind-driven circulation are equally important. Zhang et al. (2014) also found a dramatic increase in the AMOC in their model simulations of a White Mountain, but they did not report how the equatorial heat transport was different. We will note that a very much stronger AMOC is not a consistent feature of White Mountain simulations: other simulations of HadCM3 with the same height of ice sheet but using a land–sea mask of the LGM, rather than the preindustrial that we show here, do not show a large increase in their AMOC. The modeled changes to the energy budget in the simulation using an LGM mask are, however, very similar to those presented here which reiterates that changes in the AMOC are not primarily responsible for the changes in the energy budget that we see.

In ALB/TOP we see that although the boundary condition changes do imply that there is a cross-equatorial heat flux from the south to the north, the atmosphere plays no role in this. Thus, if we assume that the atmospheric cross-equatorial heat transport and the ITCZ are related, we would not expect to see any movements in the ITCZ in this experiment, despite there being a large interhemispheric energy imbalance.

Thus far we have shown that if we impose an ice sheet in the model, it can cause a change in the TOA energy balance over itself. This imbalance is then offset by compensating fluxes, remote from the ice sheet. The exact location of these is determined by the type of ice sheet forcing that is used. We summarize these results schematically in Fig. 7.

The differences between TOP and ALB that we find are not inconsistent with the results of Chiang et al. (2003) in their slab model experiments of a Green Mountain and White Plain. They found that these experiments forced an opposite signed surface response and noted that the mid latitudes responded strongest to the Green Mountain and tropics to a White Plain. This is in some ways similar to our experiments in which we find a strong response in TOP just to the south of the ice sheet in the northern midlatitudes. The experiments of Lee et al. (2015) also examined the response of the climate to ice sheet topography. They showed that there was an implied northward cross-equatorial atmospheric heat transport when the ice sheet surface was raised. This is counter to our results. If we compare our White Plain (ALB) to the White Mountain (ALB/TOP) experiments we simulate a southward heat transport in the atmosphere in response to an elevated surface. However, the model used by Lee et al. (2015) had only a reduced gravity ocean model, which cannot simulate any changes in ocean heat transport. In our experiments the ocean heat transport responds strongly to a change in the albedo, and can be the dominant term, which suggests that neglecting the ocean is a serious omission. Interestingly, just south of the ice sheet Lee et al. (2015) simulate anomalous southward atmospheric heat transports in response to ice sheet topography, which is consistent with our experiments.

So far we have used an ice sheet that is at its 21ka extent. Such an ice sheet is rather unrepresentative of the state of the ice sheet for much of any glacial period. During these periods the ice sheet will be smaller in both topographic height and extent (Kleman et al. 2013). We have seen that the effects of the topography and albedo of an ice sheet are quite different. Therefore we shall now examine what role these mechanisms play at intermediate ice sheet heights and extents to understand the interplay between these two effects.

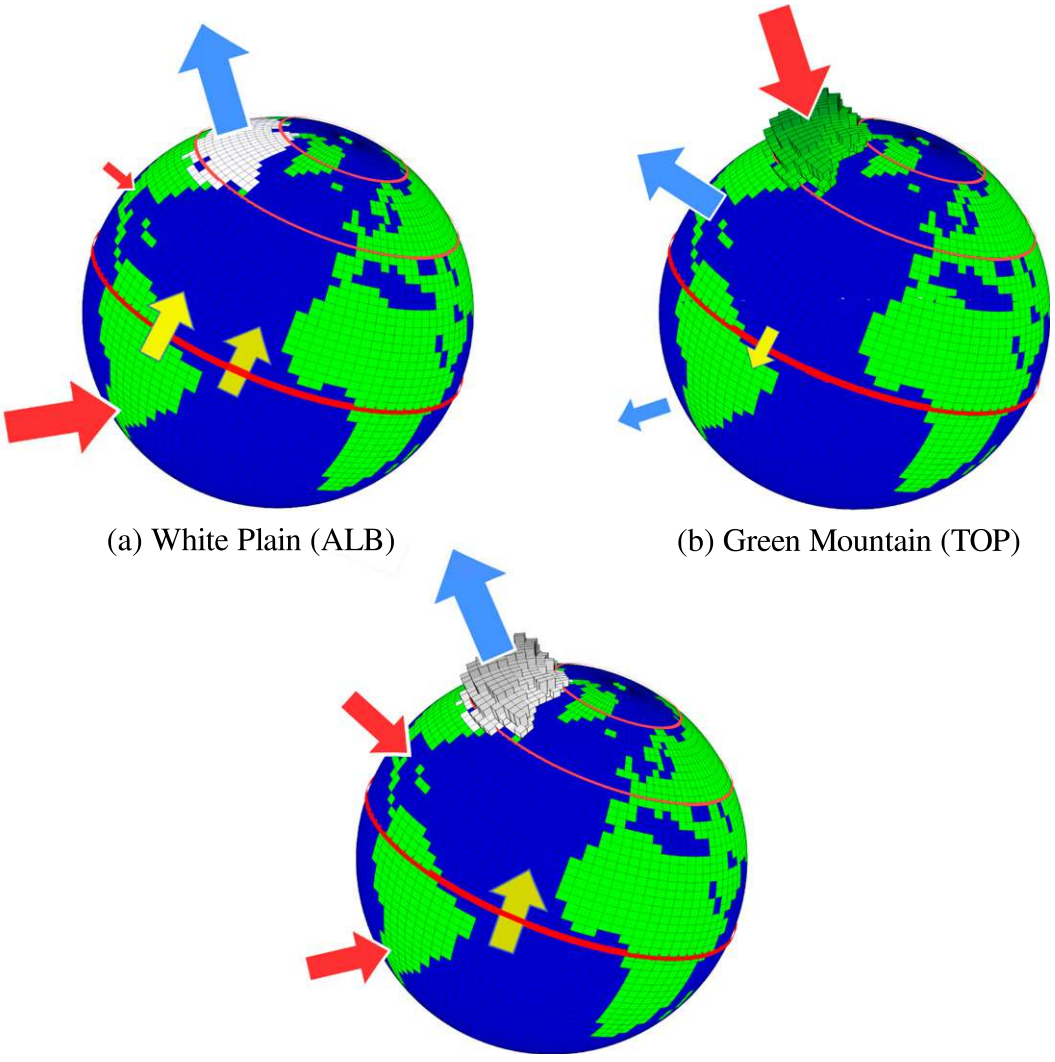

FIG. 7. Cartoon of TOA energy flux and inferred cross-equatorial heat fluxes in the three experiments. Red lines indicate the limits of the regions NTrop and SHem. Yellow arrows beneath the red lines indicate ocean heat transports; those above indicate atmospheric heat transports.

5. Global TOA energy budget for 21 ka to 6 ka ice sheets

We showed in section 4 that in experiment ALB the increase in the outgoing TOA radiation caused by the ice sheet was balanced by an increase in the incoming radiation in the SH and, to a lesser extent, in the northern tropics. Figure 8a shows that as we reduce the area of the ice sheet from its largest extent, at 21ka, the outgoing radiation anomaly is reduced and that this is balanced by a decreasing incoming radiation anomaly in the SH. The implied northward atmospheric heat transport decreases with the decreasing ice sheet albedo and remains as a nearly constant fraction of the SH TOA radiation anomaly, as does the ocean heat transport. This indicates that the share of the total northward heat transport carried by the atmosphere does not depend upon the size of the ice sheet.

Since the area of the ice sheet does not vary linearly in time over the course of the deglaciation we also plot the SH radiation anomaly as a function of the ice sheet area in Fig. 9d. We see in the red squares of the ALB experiment that the change in the incoming radiation anomaly varies linearly with the ice sheet area, with a larger ice sheet area giving rise to a larger radiation anomaly. We find, therefore, that with an intermediate area to the ice sheet the climate's response is very similar to that with the largest ice sheet, but that the amplitude of the response is reduced.

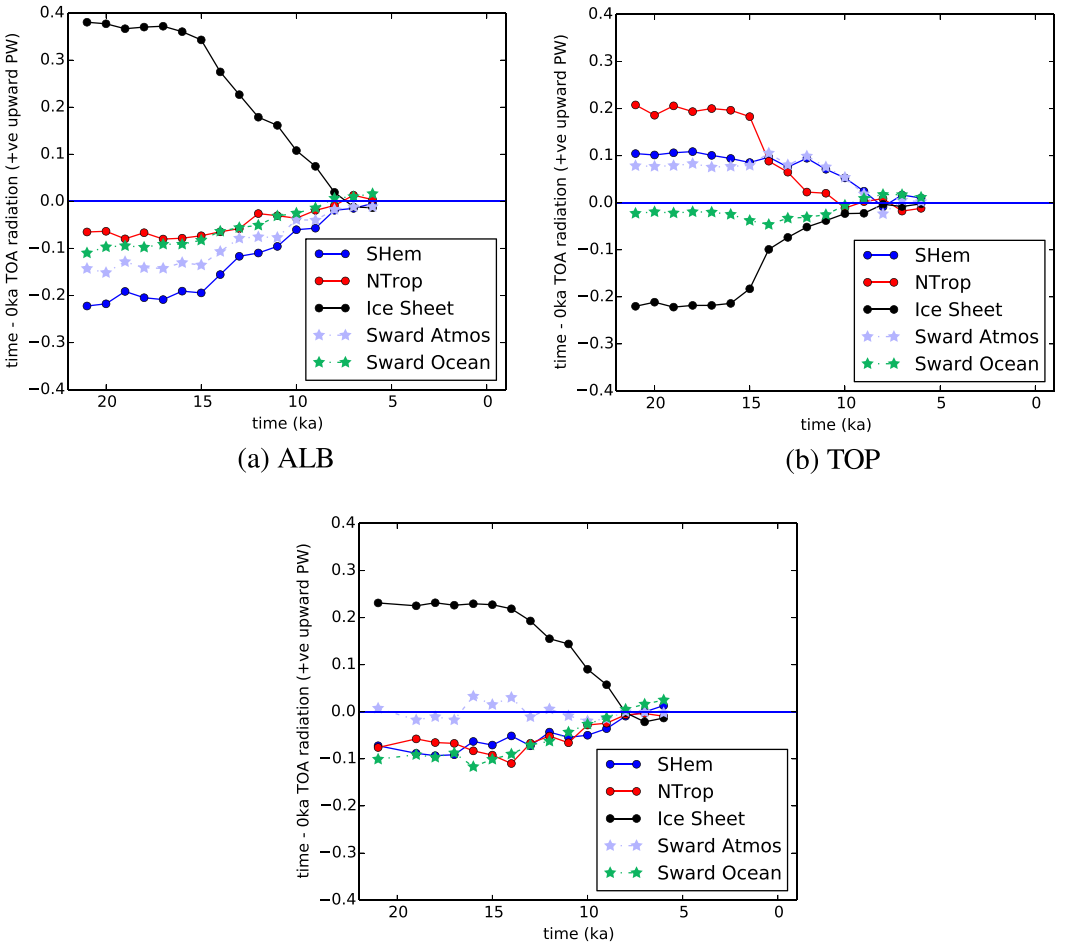

FIG. 8. Zonally integrated TOA radiation from 21 ka until 6 ka. The net TOA flux is plotted in a number of latitude bands; see text and legend for details. We plot the differences compared to the preindustrial control.

We turn now to the TOP experiment. Figure 8b shows that when the ice sheet is large, from 21 ka until 15 ka, there is an incoming TOA radiation anomaly over the ice sheet that is balanced by a large outgoing TOA radiation anomaly in NTrop and a smaller outgoing energy flux in SHem. Between 15 ka and 14 ka, there is a large decrease in the outgoing energy flux in NTrop, and a decrease in the incoming energy flux over the ice sheet. The magnitude of the energy flux out of the TOA in SHem, however, remains the same size at this time. SHem does not begin to decrease until 12 ka having been fairly constant from 21 ka until 12 ka. We find that the atmosphere is responsible for almost all of the northward cross-equatorial energy transport for all states of the ice sheet. The different behavior of the SHem and NTrop TOA energy fluxes suggests that these two features are controlled by different mechanisms.

Figures 9a and 9c show how the energy fluxes vary with respect to the size of the ice sheet. In Fig. 9a we see that the NTrop energy flux increases roughly monotonically with increasing height of the ice sheet. The rapid jump that was apparent in the time series for this quantity between 15 ka and 14 ka is due to the large change in the average height of the ice sheet at this time, not to a nonlinearity in the relationship between NTrop and ice sheet height. This can be seen more clearly when the faint markers, which indicate experiments using a different ice sheet topography reconstruction, are incorporated.

Figure 9c shows how the SHem outgoing energy flux varies. This flux increases monotonically from zero until the ice sheet has an average height of around 300 m, at which point it remains constant regardless of the increasing ice sheet height. This threshold is reached at around 12 ka in our simulations. The cause of the SHem energy flux in these simulations is an increased outgoing flux from the central/eastern tropical Pacific (Fig. 5b). As the ice sheet grows, the model's South Pacific

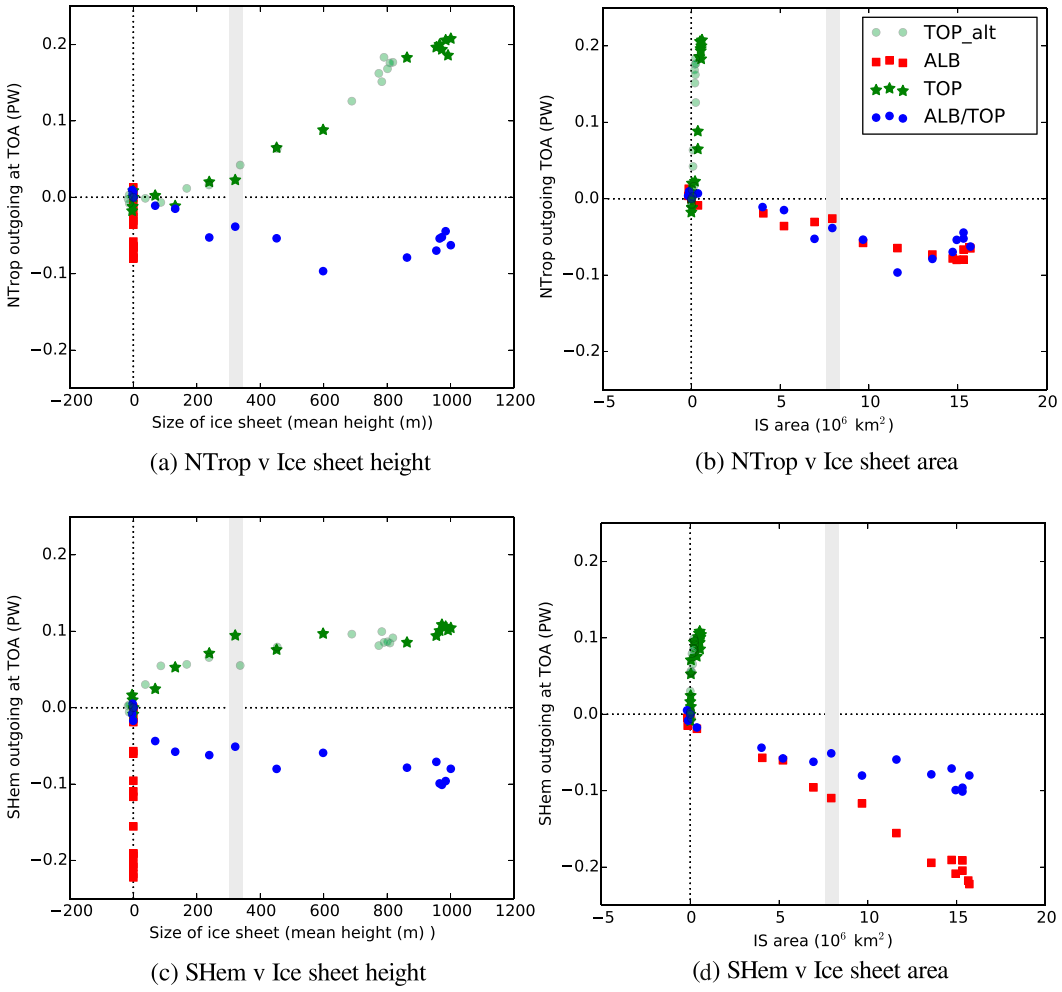

FIG. 9. Zonally integrated TOA radiation compared to ice sheet height and area. We plot the NTrop and SHem energy fluxes against the mean height and total area of the ice sheet. We plot the differences compared to the preindustrial control. Gray bands show the area and mean height of the ice sheet at 12 ka.

convergence zone moves west and south, away from east Pacific, giving rise to an anomalous TOA energy flux. Increasing ice sheet height is only able to shift the SPCZ so far, a distance that is reached at an ice sheet of about 300 m. Beyond this the SH climate changes very little, and maps of the SH from 21ka to 12 ka are very similar (not shown). The atmospheric component of the cross-equatorial heat transport is always the largest term. We find that although there is little change in the cross-equatorial heat transport there are large changes in the strength of the AMOC. In all of these simulations the AMOC varies from 16.5 to 18.5 Sv. The strongest AMOC is at intermediate ice sheet heights of around 200 m, the weakest when the ice sheet is largest. We reiterate, however, that this has little impact on the heat transport across the equator.

In ALB/TOP we see that both the SHem and NTrop energy flux are always an incoming energy flux to balance the outgoing anomaly over the ice sheet. Both SHem and NTrop steadily decrease in magnitude as the ice sheet diminishes over the deglaciation, and the relative importance of each term remains about the same.

From Figs. 9c and 9d it does not appear that SHem responds more to albedo or topography changes: the energy anomaly varies roughly linearly with both ice sheet area and height. This is not altogether surprising since area and height are of course related. Unlike TOP we do not, however, see any threshold-like behavior when the ice sheet reaches a certain height. This indicates that the nature of the climate's response to raised topography does depend upon the type of surface that is being raised.

The NTrop flux in ALB/TOP steadily decreases in magnitude over the deglaciation. Such a decrease was also seen in TOP, but recall that in TOP NTrop was an outgoing radiative flux whereas in ALB/TOP it is an incoming anomaly. There is no clearly stronger relationship between NTrop and either the ice sheet area

or the mean ice sheet height. Experiment TOP showed a clear relationship between the NTrop flux and ice sheet height, and we find that in ALB/TOP not only is the relationship of the opposite sign, but it is also weaker than in TOP. This again shows that the type of surface that is being raised as an ice sheet has a crucial impact on the climate's response.

We find that the atmospheric cross-equatorial heat flux is negligible throughout the deglaciation in ALB/TOP. Therefore, contrary to both ALB and TOP, the ocean is responsible for the majority of the cross-equatorial heat flux. We highlighted this result in the preceding section examining the 21ka simulations, and it is interesting to note that at no point do we find that the atmosphere plays a role in the transporting heat across the equator. The cross-equatorial ocean heat transport increases roughly monotonically with the increasing ice sheet. The AMOC, however, does not increase monotonically with increasing ice sheet size. Between its 14 ka and 15 ka size there is a rapid increase in the strength of the AMOC by around 4 Sv. We do not see any similarly rapid changes in any of the time series plotted in Fig. 8c, which indicates that the AMOC is not important, not even in determining the ocean heat transport in this experiment.

Our experiments show that the relationships we found in section 4 and summarized in Fig. 7 do not change much as we vary the size of the ice sheet. Except in experiment TOP, where the SHem flux increased with increasing topography only until the ice sheet reached an average height of about 300 m, the relationship between the size of the ice sheet and the various fluxes is roughly linear. This suggests that ice sheet geometry does not force any abrupt or nonlinear behavior in the global climate.

6. Conclusions and discussion

In this study we have shown how the TOA energy budget changes in response to the imposition of an ice sheet.

We showed that taken in isolation the effect of albedo and ice sheet topography are opposite over the ice sheet. When taken together, the effect of albedo alone is closest to the combined effect; however, there are still significant differences. Increasing the albedo of the surface (a White Plain; experiment ALB) increases the outgoing shortwave radiation over the ice sheet, and although there is also a small decrease in the OLR this is not enough to balance the increase in outgoing shortwave radiation. The increased outgoing shortwave radiation is almost entirely due to the change in the surface albedo, with a negligible change in the atmospheric contribution to the albedo. Increasing only the surface topography (a Green Mountain; experiment TOP) leads to a decrease in the net outgoing radiation (i.e., an increase in the net incoming radiation) over the ice sheet. This is the result of decreases in both the longwave and shortwave outgoing radiation. The decrease in the shortwave radiation results from a decrease in the atmospheric contribution to the planetary albedo. Changing both albedo and topography together (a White Mountain; experiment ALB/TOP) causes an increase in the net outgoing radiation over the ice sheet. The magnitude of this change is remarkably similar to the change in ALB; however, there are additional feedbacks in this experiment. In ALB/TOP the increase in the outgoing shortwave radiation is larger than in ALB as is the corresponding decrease in the OLR. Furthermore, in ALB the change in the planetary albedo, and hence the outgoing shortwave radiation, was almost entirely a response to the changing surface albedo. In ALB/TOP, however, there is a significant decrease in the atmospheric contribution to the albedo, which is then offset by an additional increase in the surface albedo. Therefore, although the net change in the TOA radiation is remarkably similar between the ALB and ALB/TOP, the means by which this change is achieved is rather different. In none of of our experiments does the sea ice extent change sufficiently to affect our results.

Examining the global energy balance in the three experiments also shows the importance in considering all parts of the ice sheet forcing. These results are summarized in Fig. 7. With only the effect of albedo considered, the outgoing TOA energy anomaly over the ice sheet is predominantly balanced by an incoming anomaly in the SH. This is then carried across the equator by both the atmosphere and the ocean in roughly equal proportions. A Green Mountain, by contrast, not only forces an incoming radiation anomaly over the ice sheet but also leads to a balance predominantly by an outgoing radiation flux in the NH to the south of the ice sheet. There is a small outgoing energy flux in the SH and the cross-equatorial energy flux is almost entirely carried by the atmosphere. When combined as a White Mountain we find that the outgoing energy anomaly over the ice sheet is balanced by energy fluxes into the SH, as in the White Plain, and into the NH south of the ice sheet, the location favored by a Green Mountain. The cross-equatorial energy flux in this case is carried almost entirely by the ocean, unlike either the White Plain or the Green Mountain. A possible explanation for this is that the topography and the albedo force opposing atmospheric heat transports across the equator, with the net result that there is no atmospheric heat transport. Therefore the necessary cross-equatorial heat transport, needed to balance the

global TOA energy budget, can only be carried by the ocean.

We also examined how the balance of TOA energy terms evolve as the ice sheet itself evolves using a reconstruction of the last deglaciation (Peltier 2004). We find that in the case of a White Plain, both the size of the outgoing radiation anomaly over the ice sheet and the compensating incoming flux over the SH vary linearly with the area of the ice sheet. In the case of a Green Mountain the outgoing energy flux in the NH, to the south of the ice sheet, increases monotonically with the increasing height of the ice sheet. The outgoing SH energy flux, however, increases with increasing ice sheet height until the ice sheet reaches an average height of about 300 m, at which point the size of this flux plateaus out and remains the same regardless of the ice sheet height. Thus we find that the cross-equatorial heat transport in this experiment is constant when the ice sheet height is between its peak and 300 m, which in terms of time is from 21ka until about 12 ka. With a White Mountain we find that both the SH energy flux and the flux to the south of the ice sheet vary approximately linearly with the size of the ice sheet. We find that the sensitivity of the SH energy flux to varying albedo is roughly half that in the case of the White Plain. Since this flux is the source of the cross-equatorial energy flux we find a similar reduction in the sensitivity of this term to albedo. Finally, we find that the atmospheric cross-equatorial energy flux remains small at all sizes of the ice sheet, indicating that it is the ocean that is primarily responsible for transporting heat at all states of the ice sheet.

In the introduction we set as part of our motivation for examining the TOA energy balance trying to understand how the ITCZ might move in response to an ice sheet. Since it has been argued that movements in the ITCZ are in some way a requirement for transporting energy across the equator (Chiang and Bitz 2005; Kang et al. 2008, 2009; Donohoe et al. 2013; Cvijanovic and Chiang 2013), a first step to understanding the ITCZ is to understand the actual energy budget that movements in the ITCZ may be responding to. The first comment is that we do not find that imposing an ice sheet, with its concomitant impact on the TOA energy budget, necessarily implies that there is an atmospheric heat transport across the equator. In the Green Mountain case we found that a radiative flux anomaly over the ice sheet can be balanced by fluxes out of the atmosphere in the same hemisphere as the ice sheet, not therefore requiring any cross-equatorial heat fluxes. The idea that an imposed forcing in the extratropics can be offset by heat fluxes in different places is not new: Kang et al. (2008) discuss this ''compensation'' in depth. Kang et al. (2008), however, consider how different physical parameters affect this compensation. We show that this compensation can also be altered by the very nature of the forcing.

In the experiments in which a cross-equatorial heat flux is implied we do not find that this must be carried by the atmosphere. In the White Mountain we found that although the energy flux anomaly over the ice sheet implied a heat flux into the TOA in the SH, this heat flux was transported across the equator by the ocean, not by the atmosphere. In the White Plain case, although the only compensating heat flux came from the SH, the atmosphere was not solely responsible for carrying this heat across the equator. Therefore, even though all of our runs impose some change in the energy budget in the high northern latitudes, they do not require either a cross-equatorial atmospheric heat flux or indeed a cross-equatorial heat flux by either the atmosphere or the ocean. This result is somewhat counter to results found in other studies.

The idealized studies of Kang et al. (2008), Chiang and Bitz (2005), Cvijanovic and Chiang (2013), and Lee et al. (2015) all show an atmospheric energy flux across the equator. However, these simulations all use simple slab ocean models, in which the ocean heat transport is fixed and cannot adjust to the forcing. Therefore, in these experiments the only way that the climate can affect an anomalous cross-equatorial heat flux is in the atmosphere. It comes with little surprise, therefore, that in all of these experiments the changes in the interhemispheric energy budget are balanced through the atmosphere. Furthermore, in the idealized simulations the forcing is imposed as some sort of perturbation to the surface energy flux, and as we have shown in our simulations, predicting the surface energy flux response to the forcing from an ice sheet is not trivial. In ALB there was a negligible change in the surface heat flux yet large changes in the climate and TOA fluxes. Over the ice sheet there were negligible changes in the surface heat flux because the increased surface albedo caused an increase in the upward shortwave radiation, but the surface also cooled, decreasing the upward sensible and latent heat fluxes. This balanced the shortwave change. Over the oceans there was little change in the heat flux from the ocean to the atmosphere (see Fig. 7). Thus it is possible to get large changes in the TOA energy budget with no change in the surface energy budget. Furthermore in TOP and ALB/TOP the large changes in the surface heat fluxes are the result of fluxes of heat from the ocean and in both cases the flux of heat is out of the ocean. However at the TOA the response to the ice sheet is of opposite sign. One must be extremely careful, therefore, in interpreting idealized model results, to take into account exactly what parameters are held fixed in the simulations

and what effect this might have when compared to simulations in which they are free parameters.

We described in the introduction how, in order to understand the climate's response to glacial forcing over a full glacial cycle, one must understand the climate's response to intermediate ice sheets. Our results show that the climate's response is mostly linear to different sizes of ice sheet even when the albedo and topography changed simultaneously. However, our White Mountain simulations assumed an ice sheet history over the deglaciation. During the glacial inception the relationship between albedo and topography was likely rather different. As has been shown by Stokes et al. (2012), before the LGM the ice sheets tended to be flatter and wider than during the deglaciation when they were taller and covered less area. Therefore during the early part of the last glacial the climate's response was likely more along the lines of a White Plain than our White Mountain simulations. This would tend to enhance the role that the atmosphere plays in transporting heat across the equator.

Our simulations can also shed light upon some of the rapid climate changes that were seen during the last glacial period. Dansgaard/Oeschger (D/O) events, when there were large and rapid Northern Hemisphere warmings but no presumed changes in the ice sheet configuration, will likely have a very similar response to our White Plain simulations. D/O events have been used as exemplars for ITCZ shifts in response to hemispheric asymmetric warming (Chiang and Bitz 2005; Kang et al. 2008, 2009). Our White Plain simulations, with their changes in their atmospheric heat transport across the equator, echo this. Heinrich events with their rapid changes in the topography of the ice sheet are likely to see an ice sheet forcing more like a White Mountain and, as we showed, the changing topography markedly changes the climate's response. Framing the climate's response to a Heinrich event in terms of a mere surface cooling is, therefore, not accurate. Many studies have already shown that changes to the atmospheric circulation are possible in Heinrich events (Hostetler et al. 1999; Jackson 2000; Roberts et al. 2014). Of course, during Heinrich events the climate is also likely to be responding to changes in the ocean circulation arising from the ice that is released from the collapsing ice sheet, which is the ultimate cause of the Heinrich event; however, changes to the ocean circulation are not likely to be the only forcing to the atmosphere.

We shall address in a follow-up study how the simulated ITCZ responds to the ice sheet forcing and how this links with the global energy budget changes we have outlined here. Results suggest that although movements in the ITCZ do imply changes in the transport of heat across the equator, the ITCZ does not necessarily move in response to changes in the global energy budget.

Inherent in many arguments arising from the analysis of a GCM is a certain circularity: frequently a proposed response to some climatic forcings is itself a forcing to the climate. Analyzing the TOA heat budget was an effort to try to break this circularity, since it is the energy entering the TOA that determines the circulation. It could be argued that if we understand the changes in the vertical energy fluxes at the TOA we can then frame our understanding of changes in the horizontal heat budget as being necessary to balance the TOA energy budget. However, even here there is a problem because, as we have seen, the atmospheric circulation, and its implied horizontal heat fluxes, can also determine the TOA energy budget. In the White Plain/ALB case, the change in the TOA energy balance was a direct radiative response to changing the albedo of the surface, therefore all other changes to the climate stemmed from this change at the TOA. In the Green Mountain/TOP case by contrast, the change in the TOA energy balance arose, in part, from changes in the planetary albedo that were caused by the thermodynamics of the atmosphere. In other words, the change in the TOA energy balance was a response to changes in the circulation, not a cause of it. Furthermore, if these same atmospheric circulation changes caused the increased transport of heat southward, the TOA energy budget changes in TOP could have been a necessary response to the altered horizontal heat transports not a cause of them. Therefore, although appealingly simple, understanding changes in the TOA radiation budget may not be as fundamental to understanding the root cause of the circulation changes as we would like.

Acknowledgments. This work was funded by a Leverhulme Trust Research Project Grant. The authors thank John Chiang, Paul Hezel, Camille Li, Kerim Nisancioglu, and Justin Wettstein for many discussions. WHGR thanks the Bjerknes Centre at University of Bergen for acting as gracious hosts while much of this work was undertaken. This work was carried out using the computational facilities of the Advanced Computing Research Centre, University of Bristol (http://www.bris.ac.uk/acrc/).

REFERENCES

Broccoli, A. J., and S. Manabe, 1987: The influence of continental ice, atmospheric CO_2, and land albedo on the climate of the last glacial maximum. *Climate Dyn.*, **1**, 87–99, doi:10.1007/BF01054478.

Chiang, J. C. H., and C. M. Bitz, 2005: Influence of high latitude ice cover on the marine intertropical convergence zone. *Climate Dyn.*, **25**, 477–496, doi:10.1007/s00382-005-0040-5.

——, and A. R. Friedman, 2012: Extratropical cooling, interhemispheric thermal gradients, and tropical climate

change. *Annu. Rev. Earth Planet. Sci.*, **40**, 383–412, doi:10.1146/annurev-earth-042711-105545.

——, M. Biasutti, and D. S. Battisti, 2003: Sensitivity of the Atlantic intertropical convergence zone to Last Glacial Maximum boundary conditions. *Paleoceanography*, **18**, 1094, doi:10.1029/2003PA000916.

Cook, K. H., and I. M. Held, 1988: Stationary waves of the Ice Age climate. *J. Climate*, **1**, 807–819, doi:10.1175/1520-0442(1988)001<0807:SWOTIA>2.0.CO;2.

Cvijanovic, I., and J. C. H. Chiang, 2013: Global energy budget changes to high latitude North Atlantic cooling and the tropical ITCZ response. *Climate Dyn.*, **40**, 1435–1452, doi:10.1007/s00382-012-1482-1.

Czaja, A., and J. Marshall, 2006: The partitioning of poleward heat transport between the atmosphere and ocean. *J. Atmos. Sci.*, **63**, 1498–1511, doi:10.1175/JAS3695.1.

Donohoe, A., and D. S. Battisti, 2011: Atmospheric and surface contributions to planetary albedo. *J. Climate*, **24**, 4402–4418, doi:10.1175/2011JCLI3946.1.

——, J. Marshall, D. Ferreira, and D. Mcgee, 2013: The relationship between ITCZ location and cross-equatorial atmospheric heat transport: From the seasonal cycle to the Last Glacial Maximum. *J. Climate*, **26**, 3597–3618, doi:10.1175/JCLI-D-12-00467.1.

Felzer, B., R. J. Oglesby, T. Webb III, and D. E. Hyman, 1996: Sensitivity of a general circulation model to changes in Northern Hemisphere ice sheets. *J. Geophys. Res.*, **101**, 19 077–19 092, doi:10.1029/96JD01219.

Gordon, C., C. Cooper, C. A. Senior, H. Banks, J. M. Gregory, T. C. Johns, J. F. B. Mitchell, and R. A. Wood, 2000: The simulation of SST, sea ice extents and ocean heat transports in a version of the Hadley Centre coupled model without flux adjustments. *Climate Dyn.*, **16**, 147–168, doi:10.1007/s003820050010.

Hansen, J., A. Lacis, D. Rind, G. Russell, P. Stone, I. Fung, R. Ruedy, and J. Lerner, 1984: Climate sensitivity: Analysis of feedback mechanisms. *Climate Processes and Climate Sensitivity*, *Meteor. Monogr.*, Vol. 29, Amer. Geophys. Union, 130–163, doi:10.1029/GM029p0130.

Hofer, D., C. C. Raible, A. Dehnert, and J. Kuhlemann, 2012: The impact of different glacial boundary conditions on atmospheric dynamics and precipitation in the North Atlantic region. *Climate Past*, **8**, 935–949, doi:10.5194/cp-8-935-2012.

Hostetler, S. W., P. U. Clark, P. J. Bartlein, C. Mix, and N. J. Pisias, 1999: Atmospheric transmission of North Atlantic Heinrich events. *J. Geophys. Res.*, **104**, 3947–3952, doi:10.1029/1998JD200067.

Jackson, C., 2000: Sensitivity of stationary wave amplitude to regional changes in Laurentide ice sheet topography in single-layer models of the atmosphere. *J. Geophys. Res.*, **105** (D19), 24 443–24 454, doi:10.1029/2000JD900377.

Justino, F., A. Timmermann, U. Merkel, and E. P. Souza, 2005: Synoptic reorganization of atmospheric flow during the Last Glacial Maximum. *J. Climate*, **18**, 2826–2846, doi:10.1175/JCLI3403.1.

Kageyama, M., and P. J. Valdes, 2000: Impact of the North American ice-sheet orography on the Last Glacial Maximum eddies and snowfall. *Geophys. Res. Lett.*, **27**, 1515–1518, doi:10.1029/1999GL011274.

Kang, S. M., I. M. Held, D. M. W. Frierson, and M. Zhao, 2008: The response of the ITCZ to extratropical thermal forcing: Idealized slab-ocean experiments with a GCM. *J. Climate*, **21**, 3521–3532, doi:10.1175/2007JCLI2146.1.

——, D. M. W. Frierson, and I. M. Held, 2009: The tropical response to extratropical thermal forcing in an idealized GCM: The importance of radiative feedbacks and convective parameterization. *J. Atmos. Sci.*, **66**, 2812–2827, doi:10.1175/2009JAS2924.1.

Kleman, J., J. Fastook, K. Ebert, J. Nilsson, and R. Caballero, 2013: Pre-LGM Northern Hemisphere ice sheet topography. *Climate Past*, **9**, 2365–2378, doi:10.5194/cp-9-2365-2013.

Kutzbach, J., and H. Wright, 1985: Simulation of the climate of 18,000 years BP: Results for the North American/North Atlantic/European sector and comparison with the geologic record of North America. *Quat. Sci. Rev.*, **4**, 147–187, doi:10.1016/0277-3791(85)90024-1.

Lee, S.-Y., J. C. H. Chiang, and P. Chang, 2015: Tropical Pacific response to continental ice sheet topography. *Climate Dyn.*, **44**, 2429–2446, doi:10.1007/s00382-014-2162-0.

Li, C., and D. S. Battisti, 2008: Reduced Atlantic storminess during Last Glacial Maximum: Evidence from a coupled climate model. *J. Climate*, **21**, 3561–3579, doi:10.1175/2007JCLI2166.1.

Manabe, S., and J. Broccoli, 1985: The influence of continental ice sheets on the climate of an ice age. *J. Geophys. Res.*, **90** (D1), 2167–2190, doi:10.1029/JD090iD01p02167.

Pausata, F. S. R., C. Li, J. J. Wettstein, M. Kageyama, and K. H. Nisancioglu, 2011: The key role of topography in altering North Atlantic atmospheric circulation during the last glacial period. *Climate Past*, **7**, 1089–1101, doi:10.5194/cp-7-1089-2011.

Peltier, W., 2004: Global glacial isostasy and the surface of the ice-age earth: The ICE-5G (VM2) Model and GRACE. *Annu. Rev. Earth Planet. Sci.*, **32**, 111–149, doi:10.1146/annurev.earth.32.082503.144359.

Phillipps, P. J., and I. M. Held, 1994: The response to orbital perturbations in an atmospheric model coupled to a slab ocean. *J. Climate*, **7**, 767–782, doi:10.1175/1520-0442(1994)007<0767:TRTOPI>2.0.CO;2.

Rind, D., 1987: Components of the ice age circulation. *J. Geophys. Res.*, **92** (D4), 4241–4281, doi:10.1029/JD092iD04p04241.

Roberts, W. H. G., P. J. Valdes, and A. J. Payne, 2014: Topography's crucial role in Heinrich events. *Proc. Natl. Acad. Sci. USA*, **111**, 16 688–16 693, doi:10.1073/pnas.1414882111.

Spencer, H., R. Sutton, and J. M. Slingo, 2007: El Niño in a coupled climate model: Sensitivity to changes in mean state induced by heat flux and wind stress corrections. *J. Climate*, **20**, 2273–2298, doi:10.1175/JCLI4111.1.

Stokes, C. R., L. Tarasov, and A. S. Dyke, 2012: Dynamics of the North American Ice Sheet Complex during its inception and build-up to the Last Glacial Maximum. *Quat. Sci. Rev.*, **50**, 86–104, doi:10.1016/j.quascirev.2012.07.009.

Toniazzo, T., M. Collins, and J. Brown, 2008: The variation of ENSO characteristics associated with atmospheric parameter perturbations in a coupled model. *Climate Dyn.*, **30**, 643–656, doi:10.1007/s00382-007-0313-2.

Ullman, D. J., A. N. Legrande, A. E. Carlson, F. S. Anslow, and J. M. Licciardi, 2014: Assessing the impact of Laurentide ice sheet topography on glacial climate. *Climate Past*, **10**, 487–507, doi:10.5194/cp-10-487-2014.

Yoshimori, M., and A. J. Broccoli, 2008: Equilibrium response of an atmosphere–mixed layer ocean model to different radiative forcing agents: Global and zonal mean response. *J. Climate*, **21**, 4399–4423, doi:10.1175/2008JCLI2172.1.

Zhang, X., G. Lohmann, G. Knorr, and C. Purcell, 2014: Abrupt glacial climate shifts controlled by ice sheet changes. *Nature*, **512**, 290–294, doi:10.1038/nature13592.